Mathematical Analysis of Magnetically Controlled Ferrofluid Transport for Electronic Thermal Systems

*[1]Ojo, Adetoye Solomon., [2]Nwabuzor, Peter Onyelukachukwu

[1]Department of Physics, University of Port Harcourt, PMB 5323 Choba, Nigeria

[2]Department of Physics with Electronics, University of Port Harcourt, PMB 5323 Choba, Nigeria

*Corresponding Author

DOI: https://doi.org/10.51584/IJRIAS.2026.11060273

Received: 02 July 2026; Accepted: 07 July 2026; Published: 16 July 2026

ABSTRACT

The increasing thermal demands of modern electronic devices have intensified the need for efficient and controllable heat transfer mechanisms capable of sustaining system reliability and performance. In this study, a mathematical model is developed to investigate magnetically controlled ferrofluid transport in an electronic thermal system using an electrically conducting Fe_3O_4-water nanofluid flowing through a chemically reactive porous channel. The model incorporates the combined effects of magnetohydrodynamics (MHD), thermal radiation, variable electrical conductivity, porous resistance, and species diffusion on the transport behavior of the ferrofluid. Hybrid constitutive relations are employed to evaluate the effective viscosity and thermal conductivity of the nanofluid in order to capture nanoparticle interaction effects more accurately. The governing equations for momentum, energy, and concentration transport are transformed into dimensionless form using the Brinkman model. Analytical solutions are then obtained using the Laplace transform technique to derive closed-form expressions for velocity, temperature, and concentration distributions. The influence of important dimensionless parameters, including Reynolds number, Hartmann number, Prandtl number, Schmidt number, radiation parameter, chemical reaction parameter, and nanoparticle volume fraction, is investigated in detail. The results indicate that increasing nanoparticle concentration significantly enhances thermal conductivity and temperature distribution within the electronic cooling domain, while strong magnetic fields suppress fluid velocity due to Lorentz force effects. The radiation parameter is found to influence thermal boundary layer development, whereas higher Schmidt and Prandtl numbers reduce concentration and temperature diffusion respectively. Furthermore, chemical reaction effects contribute to species depletion and flow suppression within the porous medium. The present analytical model provides valuable physical insight into coupled magneto-thermal transport mechanisms and offers a predictive framework for the design and optimization of advanced electronic cooling systems employing ferrofluid technology.

Keywords: Ferrofluid transport; Fe_3O_4 nanofluid; electronic thermal systems; magnetohydrodynamics; porous media; thermal radiation; Laplace transform; heat transfer enhancement; analytical modeling; electromagnetic flow control.

INTRODUCTION

The continuous advancement of modern electronics and micro-scale technologies has significantly increased the thermal demands placed on electronic devices and systems. High-performance processors, integrated circuits, communication devices, embedded sensors, and power electronics generate substantial amounts of heat during operation, leading to thermal instability, reduced efficiency, and shortened operational lifespan when heat dissipation is inadequate. Efficient thermal management has therefore become one of the most critical challenges in electronics engineering, energy systems, and thermal sciences. Conventional cooling fluids such as water, mineral oil, and ethylene glycol possess relatively low thermal conductivity, limiting their ability to meet the increasing cooling requirements of compact and high-power electronic systems.

To overcome these limitations, nanofluids have emerged as promising advanced heat transfer media due to their enhanced thermophysical properties. Nanofluids are engineered suspensions of nanoparticles dispersed in conventional base fluids to improve thermal conductivity and heat transfer efficiency. Since the pioneering work of Choi and Eastman (1995), nanofluids have received considerable attention because even small concentrations of nanoparticles can produce significant enhancement in thermal transport characteristics. Eastman et al. (2001) further demonstrated anomalously increased thermal conductivity in metallic nanoparticle suspensions, thereby establishing nanofluids as viable candidates for advanced cooling technologies.

Among the various classes of nanofluids, ferrofluids containing iron oxide nanoparticles have attracted significant scientific and engineering interest because of their combined thermal and magnetic properties. Ferrofluids are stable colloidal suspensions of magnetic nanoparticles dispersed in carrier fluids and can be manipulated externally using magnetic fields. This magnetic controllability offers substantial advantages in electronic thermal systems where adaptive and targeted heat transfer regulation is required. Iron oxide nanoparticles, particularly Fe_3O_4, are widely employed because of their chemical stability, strong magnetic response, low toxicity, and favorable thermal conductivity characteristics.

Experimental investigations have confirmed the excellent thermal transport capabilities of iron oxide nanofluids. Shima et al. (2010) synthesized stable aqueous and nonaqueous Fe_3O_4 nanofluids and demonstrated that thermal conductivity increases significantly with temperature and nanoparticle concentration due to enhanced Brownian motion and particle interactions. Abareshi et al. (2011) investigated the rheological behavior of α-Fe_2O_3 nanofluids and observed that nanoparticle loading strongly affects viscosity and transport characteristics. Similarly, Guo et al. (2010) experimentally reported substantial enhancement in convective heat transfer coefficients for magnetic nanofluids containing γ-Fe_2O_3 nanoparticles flowing under laminar conditions.

The interaction between magnetic fields and electrically conducting ferrofluids produces magnetohydrodynamic (MHD) effects that significantly influence fluid flow, momentum transport, and thermal boundary layer development. In electronic cooling systems, magnetic fields can be used to actively regulate heat transfer performance and fluid circulation. Hassan (2018) demonstrated that oscillatory magnetic fields modify nanoparticle alignment and aggregation mechanisms, thereby affecting both viscosity and thermal conductivity of iron oxide nanofluids. Ghadiri et al. (2015) further showed experimentally that ferrofluids flowing through mini-channel heat sinks under magnetic fields exhibit enhanced hydrothermal performance and improved cooling efficiency suitable for compact electronic devices.

In addition to magnetic effects, thermal radiation and porous medium transport play important roles in electronic thermal systems operating under high-temperature conditions. Thermal radiation contributes significantly to heat transfer in confined thermal environments, while porous structures are frequently encountered in heat exchangers, microchannel cooling systems, catalytic devices, and porous electronic substrates. The radiative heat transfer approximation developed by Cogley et al. (1968) remains one of the most widely adopted models for optically thin radiative transport in thermal fluid systems. Moreover, variable electrical conductivity effects have been shown to influence electromagnetic damping and Lorentz force distributions in conducting fluids subjected to magnetic fields.

Several analytical and numerical studies have been conducted on ferrofluid transport phenomena in recent years. Sheikholeslami (2019) analyzed entropy generation and MHD ferrofluid flow in porous cavities and concluded that Lorentz forces significantly affect velocity suppression and thermal distribution. Farooq et al. (2023) investigated Fe_3O_4–H_2O nanofluid flow over rotating disks and observed substantial changes in thermal and hydrodynamic boundary layers under magnetic influences. Although these investigations provide valuable insight into ferrofluid transport behavior, many existing studies rely predominantly on numerical approaches such as finite difference, finite element, and Runge–Kutta techniques. While numerical simulations are effective for approximate solutions, they often provide limited analytical understanding of the coupled nonlinear transport mechanisms governing ferrofluid behavior in electronic thermal systems.

Furthermore, only limited attention has been devoted to the simultaneous incorporation of porous medium resistance, thermal radiation, variable electrical conductivity, and chemically reactive species transport within a unified analytical framework. The combined interaction of these physical mechanisms is highly relevant in advanced electronic cooling systems where electromagnetic control, thermal diffusion, and reactive transport processes coexist.

Motivated by these limitations, the present study develops a comprehensive mathematical model for magnetically controlled ferrofluid transport in electronic thermal systems using Fe_3O_4-water nanofluid flowing through a chemically reactive porous channel. The governing equations describing momentum, energy, and concentration transport are formulated under magnetohydrodynamic assumptions and transformed into dimensionless form using the Brinkman model. Analytical solutions are subsequently obtained using the Laplace transform technique to derive closed-form expressions for velocity, temperature, and concentration distributions.

The novelty of this work lies in the integration of hybrid thermophysical property models together with variable electrical conductivity, thermal radiation, porous medium resistance, and chemical reaction effects within a unified analytical framework. The results are expected to provide deeper physical understanding and practical design guidance for advanced ferrofluid-based electronic cooling technologies, electromagnetic thermal regulation systems, and next-generation heat transfer devices.

Governing Equations

The transport behavior of the Fe_3O_4–water ferrofluid within the electronic thermal system is governed by the fundamental principles of conservation of mass, momentum, energy, and species concentration. The present model considers the combined influence of magnetohydrodynamics (MHD), thermal radiation, porous medium resistance, and chemical reaction effects on the unsteady flow of the electrically conducting ferrofluid. Appropriate thermophysical relations are employed to evaluate the effective properties of the nanofluid. Based on these assumptions, the governing equations describing the velocity, temperature, and concentration fields are formulated as follows.

Continuity Equation

For an incompressible ferrofluid,

$$\nabla . V = 0 \tag{1}$$

For one–dimensional flow along the x-direction, equation (1) becomes

$$\frac{\partial u}{\partial x} + \frac{\partial v}{\partial y} = 0 \tag{2}$$

Momentum Equation

Using the Navier–Stokes equation with magnetic and porous medium effects,

$$\rho_{nf}\left(\frac{\partial u}{\partial t}\right) = \mu_{nf}\frac{\partial^2 u}{\partial y^2} - \sigma_{nf} B_0^2 u - \frac{\mu_{nf}}{K}u \tag{3}$$

Energy Equation

The dimensional energy equation including thermal radiation becomes

$$\left(\rho C_P\right)_{nf}\frac{\partial T}{\partial t} = K_{nf}\frac{\partial^2 T}{\partial y^2} - \frac{\partial q_r}{\partial y} \tag{4}$$

ISSN No. 2454-6194 | DOI: 10.51584/IJRIAS |Volume XI Issue VI June 2026

Concentration Equation

Including chemical reaction effects,

$$\frac{\partial C}{\partial t} = D\frac{\partial^2 C}{\partial y^2} - K_r\left(C - C_\infty\right) \tag{5}$$

Where, ρ_{nf} = effective density of ferrofluid, μ_{nf} = effective viscosity, σ_{nf} = electrical conductivity, D = mass diffusivity, k_r = chemical reaction parameter, B_0 = applied magnetic field, K = permeability of porous medium.

As stated by Cogley et al. (1968), the radiation impact on an optically dense model, in which the thermal layer becomes exceedingly thick, can be expressed as follows: by employing the Rosseland approximation (q_r)

$$\frac{\partial q_r}{\partial r} = -\frac{4K_B}{3\alpha}\frac{\partial T^4}{\partial r} \tag{6}$$

This is where the absorption coefficient α is defined and K_B stands for the Stefan-Boltzmann constant. If the temperature gradient within the nanofluid flow is so tiny that T^4 is a linear function of temperature, then... To do this, we extend T^4 in a Taylor series around T_∞ and exclude terms of higher order; this leads to the following expression:

$$T^4 = 4T_\infty^3 T - 3T_\infty^4 \tag{7}$$

Sequel to the diminutively change in temperature equation and incompressible fluid of equation (7) is differentiated with respect to y,

$$\frac{\partial T^4}{\partial y} = 4T_\infty^3\frac{\partial T}{\partial y} \tag{8}$$

Substitute into radiation heat flux equation,

$$q_r = \frac{16\sigma^* T_\infty^3}{3k^*}\frac{\partial T}{\partial y} \tag{9}$$

Differentiate again,

$$\frac{\partial q_r}{\partial y} = -\frac{16\sigma^* T_\infty^3}{3k^*}\frac{\partial^2 T}{\partial y^2} \tag{10}$$

Substituting equation (10) into the energy equation (4) gives

$$\left(\rho C_P\right)_{nf}\frac{\partial T}{\partial t} = \left(k_{nf} + \frac{16\sigma^* T_\infty^3}{3k^*}\right)\frac{\partial^2 T}{\partial y^2} \tag{11}$$

Effective Thermophysical Properties

The thermophysical properties of the ferrofluid significantly influence the heat and momentum transport within the electronic thermal system. In the present study, Fe_3O_4 nanoparticles are dispersed in water to enhance the thermal performance of the base fluid. The effective density, viscosity, thermal conductivity, heat capacity and electrical conductivity of the nanofluid are evaluated using appropriate constitutive relations. These effective property models are presented as follows.

ISSN No. 2454-6194 | DOI: 10.51584/IJRIAS |Volume XI Issue VI June 2026

Effective Density

$$\rho_{nf} = (1-\phi)\rho_f + \phi\rho_s \tag{12}$$

Effective Heat Capacity

$$(C_P)_{nf} = (1-\phi)(\rho C_P)_f + \phi(\rho C_P)_s \tag{13}$$

Effective Dynamic Viscosity

Using Brinkman model,

$$\mu_{nf} = \frac{\mu_f}{(1-\phi)^{2.5}} \tag{14}$$

Effective Thermal Conductivity

Using Maxwell model,

$$k_{nf} = k_f \left[\frac{k_s + 2k_f - 2\phi(k_f - k_s)}{k_s + 2k_f + \phi(k_f - k_s)} \right] \tag{15}$$

Effective Electrical Conductivity

$$\sigma_{nf} = \sigma_f \left[1 + \frac{3(\sigma_s - \sigma_f)\phi}{\sigma_s + 2\sigma_f - (\sigma_s - \sigma_f)\phi} \right] \tag{16}$$

Dimensional Analysis

The dimensional homogeneity that will enable the easy tackling of the problem of the governing nanofluid equations is stated as

$$u^* = \frac{u}{U_0}, y^* = \frac{y}{L}, \theta = \frac{tU_0}{L}, \theta = \frac{T - T_\infty}{T_w - T_\infty}, \psi = \frac{C - C_\infty}{C_w - C_\infty}, M = \frac{\sigma_{nf} B_0^2 L}{\rho_{nf} U_0}$$
$$\mathrm{Re} = \frac{\rho_{nf} U_0 L}{\mu_{nf}}, \mathrm{Pr} = \frac{\mu C_P}{k}, Sc = \frac{V}{D}, Rd = \frac{16\sigma^* T_\infty^3}{3kk^*}, Da = \frac{k}{L^2}, \gamma = \frac{k_r L}{U_0}$$

Transforming equation (3), (5) and (11) in dimensionless form, the modelled equations can be expressed as

$$\frac{\partial u}{\partial t} = \frac{1}{\mathrm{Re}} \frac{\partial^2 u}{\partial y^2} - \left[M + \frac{1}{Da} \right] u \tag{17}$$

$$\frac{\partial \theta}{\partial t} = \frac{1 + Rd}{\mathrm{Pr}} \frac{\partial^2 \theta}{\partial y^2} \tag{18}$$

$$\frac{\partial \psi}{\partial t} = \frac{1}{Sc}\frac{\partial^2 \psi}{\partial y^2} - \gamma \psi \qquad (19)$$

In which the Reynolds number represented by Re, the Prandtl number represented as Pr, the Schmidt number represented as Sc, the dimensionless radiation parameter which is represented as Rd, Da is Darcy number (porosity parameter), γ is chemical reaction parameter and ϕ as nanoparticle volume fraction.

Applying boundary conditions

Initially,

$$\begin{aligned} u(y,0) &= 0 \\ \theta(y,0) &= 0 \\ \psi(y,0) &= 0 \end{aligned} \qquad (20)$$

At the channel wall,

$$\begin{aligned} u(y,t) &= 1 \\ \theta(y,t) &= 1 \\ \psi(y,t) &= 1 \end{aligned} \qquad (21)$$

As $y \to \infty$ thus, $u \to 0,\ \theta \to 0,\ \psi \to 0$

Solution Of Momentum Equation Using Laplace Transform

Take Laplace transform of equation (17)

$$L\left[\frac{\partial u}{\partial t}\right] = s\bar{u} - u(y,0) \qquad (22)$$

Applying equation (20) initial boundary condition, since $u(y,0) - 0$ equation (22) becomes

$$s\bar{u} = \frac{1}{\mathrm{Re}}\frac{\partial^2 \bar{u}}{\partial y^2} - \left[M + \frac{1}{Da}\right]\bar{u} \qquad (23)$$

Multiply equation (23) by Re, it implies

$$\frac{\partial^2 \bar{u}}{\partial y^2} - \mathrm{Re}\left[s + M + \frac{1}{Da}\right]\bar{u} = 0 \qquad (24)$$

Let

$$\lambda^2 = \mathrm{Re}\left[s + M + \frac{1}{Da}\right] \qquad (25)$$

Substituting equation (25) into (24) it gives,

$$\frac{\partial^2 u}{\partial y^2} - \lambda^2 \bar{u} = 0 \qquad (26)$$

Let equation (26) reduce to characteristic equation

ISSN No. 2454-6194 | DOI: 10.51584/IJRIAS |Volume XI Issue VI June 2026

$$m^2 - \lambda^2 = 0 \tag{27}$$

Thus, $m = \pm\lambda$, the general solution for equation (27) gives

$$\bar{u} = Ae^{\lambda y} + Be^{-\lambda y} \tag{28}$$

Since velocity must remain finite $y \to \infty$, then A = 0 equation (28) becomes

$$\bar{u} = Be^{-\lambda y} \tag{29}$$

Using wall condition, $u(0,t) = 1$, taking Laplace transform of equation (29) it gives

$$\bar{u}(0,s) = \frac{1}{s} \tag{30}$$

Hence,

$$B = \frac{1}{s} \tag{31}$$

Therefore, substituting equation (25) and (31) into equation (29) it results

$$\bar{u}(y,s) = \frac{1}{s} e^{-y\sqrt{\mathrm{Re}\left[s+M+\frac{1}{Da}\right]}} \tag{32}$$

Solution Of Energy Equation

Take Laplace transform of equation (18) it implies

$$\frac{\partial^2 \bar{\theta}}{\partial y^2} - \frac{\Pr s}{1+Rd}\bar{\theta} = 0 \tag{33}$$

Let

$$\beta^2 = \frac{\Pr s}{1+Rd} \tag{34}$$

Substitute equation (34) into equation (33)

$$\frac{\partial^2 \bar{\theta}}{\partial y^2} - \beta^2 \bar{\theta} = 0 \tag{35}$$

General solution of equation (35) implies

$$\bar{\theta} = Ce^{\beta y} + De^{-\beta y} \tag{36}$$

Since temperature remains bounded $C = 0$

Thus,

$$\bar{\theta} = De^{-\beta y} \tag{37}$$

ISSN No. 2454-6194 | DOI: 10.51584/IJRIAS |Volume XI Issue VI June 2026

Using wall condition, $\theta(0,t)=1$, taking Laplace transform of equation (37) it gives

$$\bar{\theta}(0,s)=\frac{1}{s} \tag{38}$$

Hence,

$$D=\frac{1}{s} \tag{39}$$

Substituting equation (34) and (39) into equation (37) it results

$$\bar{\theta}(y,s)=\frac{1}{s}e^{-y\sqrt{\frac{\Pr s}{1+Rd}}} \tag{40}$$

Solution Of Concentration Equation

Take Laplace transform of equation 19 it results

$$\frac{\partial^2\bar{\psi}}{\partial y^2}-Sc(s+\gamma)\bar{\psi}=0 \tag{41}$$

Let

$$\eta^2=Sc(s+\gamma) \tag{42}$$

Inputting equation (42) into (41) it gives

$$\frac{\partial^2\bar{\psi}}{\partial y^2}-\eta^2\bar{\psi}=0 \tag{43}$$

Solution of equation (43) gives

$$\bar{\psi}=Ee^{\eta y}+Fe^{-\eta y} \tag{44}$$

Applying boundedness condition into equation (44), $E=0$.

Thus,

$$\bar{\psi}=Fe^{-\eta y} \tag{45}$$

Using wall condition, $\psi(0,t)=1$, taking Laplace transform of equation (45) it gives

$$\bar{\psi}(0,s)=\frac{1}{s} \tag{46}$$

Therefore,

$$F=\frac{1}{s} \tag{47}$$

Substituting equation (42) and (46) into equation (44) results

$$\bar{\psi}(y,s)=\frac{1}{s}e^{-y\sqrt{Sc(s+\gamma)}} \tag{48}$$

Solution of equation (32), (40) and (48) yields:

$$u(y,t)=e^{-\left[M+\frac{1}{Da}\right]t}erfc\left(\frac{y\sqrt{\mathrm{Re}}}{2\sqrt{t}}\right) \tag{49}$$

$$\theta(y,t)=erfc\left(\frac{y}{2}\sqrt{\frac{\mathrm{Pr}}{(1+Rd)t}}\right) \tag{50}$$

$$\psi(y,t)=e^{-\gamma t}erfc\left(\frac{y\sqrt{Sc}}{2\sqrt{t}}\right) \tag{51}$$

Engineering Application

The effective viscosity and thermal conductivity models were combined to capture the intrinsic thermo-physical characteristics of the Fe_3O_4–water ferrofluid employed in the present electronic thermal system. The effective thermal conductivity model provides a realistic representation of the enhanced heat transfer capability of the ferrofluid, which is essential for efficient thermal regulation, improved cooling performance, and optimal design of advanced electronic heat management systems. Similarly, the effective viscosity model accounts for the influence of nanoparticle concentration on the flow behavior of the ferrofluid, thereby affecting fluid circulation, momentum transport, and pumping characteristics under both laminar and magnetically controlled flow conditions.

The interaction between the electrically conducting Fe_3O_4–water ferrofluid and the channel surface generates a resistive force known as skin friction. This phenomenon arises due to the viscous effects associated with the relative motion between the ferrofluid and the solid boundary under the influence of magnetic and porous medium effects. In electronic thermal systems, skin friction plays an important role in determining wall shear stress, flow resistance, and pumping power requirements within the cooling channel. Therefore, the skin friction coefficient for the present ferrofluid transport model can be obtained from the velocity solution given in equation (49).

$$\left.\frac{\partial u}{\partial y}\right|_{y=0}=-\frac{\sqrt{\mathrm{Re}}}{\sqrt{\pi t}}e^{-\left[M+\frac{1}{Da}\right]t} \tag{52}$$

Thus, the skin friction coefficient becomes

$$\tau=-\frac{\mu_{nf}}{\rho U_0^2}e^{-\left[M+\frac{1}{Da}\right]t} \tag{53}$$

The Nusselt number represents the ratio of convective heat transfer to conductive heat transfer within the ferrofluid flow system. It provides a quantitative measure of the thermal transport enhancement at the fluid–solid interface and is widely used in the analysis of heat transfer performance in electronic cooling applications. In the present magnetically controlled Fe_3O_4–water ferrofluid model, the Nusselt number characterizes the influence of thermal radiation, nanoparticle concentration, and fluid motion on the rate of heat transfer at the channel surface. Hence, the local Nusselt number for the present study can be obtained from the temperature distribution given in equation (50).

$$\left.\frac{\partial\theta}{\partial y}\right|_{y=0} = -\frac{1}{\sqrt{\pi}}\sqrt{\frac{\Pr}{(1+Rd)t}} \tag{54}$$

$$Nu = \frac{1}{\sqrt{\pi}}\sqrt{\frac{\Pr}{(1+Rd)t}} \tag{55}$$

The Sherwood number is a dimensionless parameter used to characterize the rate of mass transfer within the ferrofluid flow system. It represents the ratio of convective mass transfer to diffusive mass transfer at the fluid boundary surface. In the present study, the Sherwood number describes the influence of nanoparticle diffusion, chemical reaction, and porous medium effects on species transport within the magnetically controlled Fe_3O_4–water ferrofluid. Therefore, the Sherwood number for the present electronic thermal system can be obtained from the concentration distribution presented in equation (51).

$$\left.\frac{\partial\psi}{\partial y}\right|_{y=0} = -e^{-\gamma t}\frac{\sqrt{Sc}}{\sqrt{\pi t}} \tag{56}$$

$$Sh = e^{-\gamma t}\frac{\sqrt{Sc}}{\sqrt{\pi t}} \tag{57}$$

RESULTS AND DISCUSSIONS

The effects of the governing thermo-physical and transport parameters on the magnetically controlled Fe_3O_4–water ferrofluid model for electronic thermal systems are presented in this section. Equations (49) - (51), together with the associated initial and boundary conditions given in equations (20) and (21), were solved analytically using the Laplace transform technique and evaluated numerically through the Inverse Laplace Transform approach. The obtained results are illustrated graphically in Figures 1 - 14 to describe the influence of magnetic field strength, thermal radiation, porous medium resistance, chemical reaction, and nanoparticle transport on the velocity, temperature, and concentration profiles within the ferrofluid cooling channel. The graphical results further demonstrate the thermal enhancement capability and flow control characteristics of the Fe_3O_4–water ferrofluid in advanced electronic cooling applications.

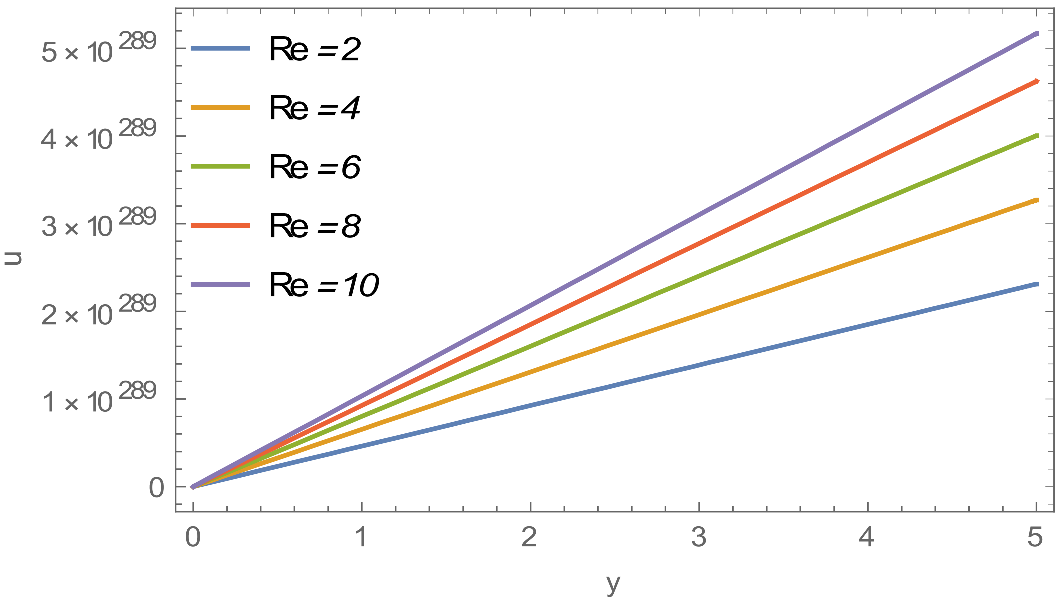

ISSN No. 2454-6194 | DOI: 10.51584/IJRIAS |Volume XI Issue VI June 2026

Figure 1: Velocity profile u against boundary layer y of electronic thermal system varying Reynolds number (Re) when M = 1.5, Da = 1.8, erfc = 0.1.

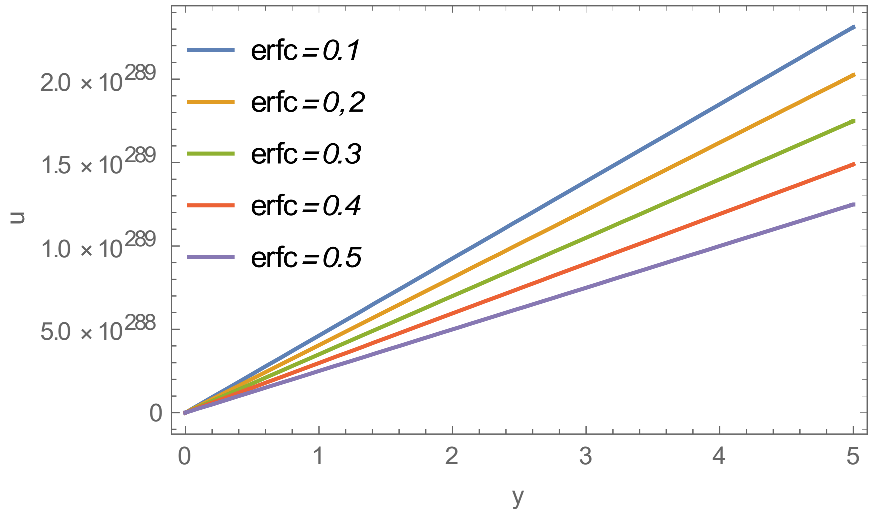

Figure 2: Velocity profile u against boundary layer y of electronic thermal system varying complementary error function (erfc) when M = 1.5, Da = 1.8, Re = 2.

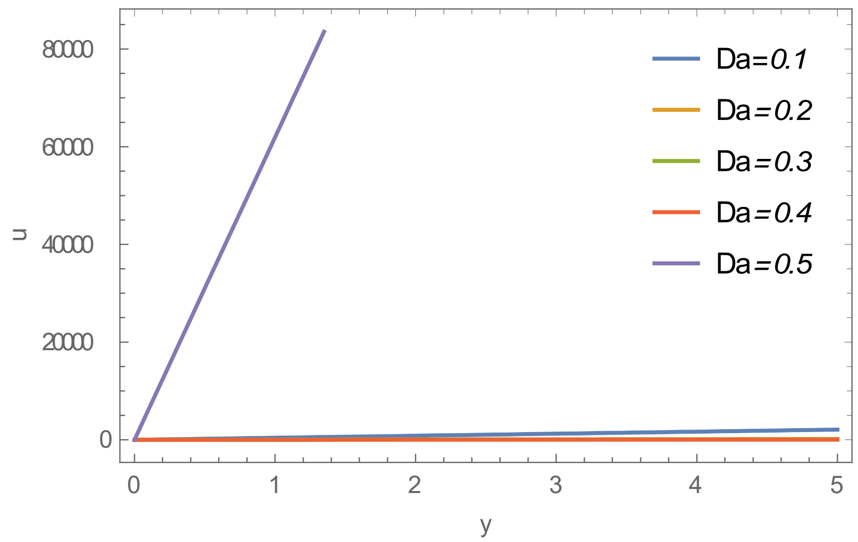

Figure 3: Velocity profile u against boundary layer y of electronic thermal system varying Darcy number (Da) when M = 1.5, erfc = 0.1, Re = 2.

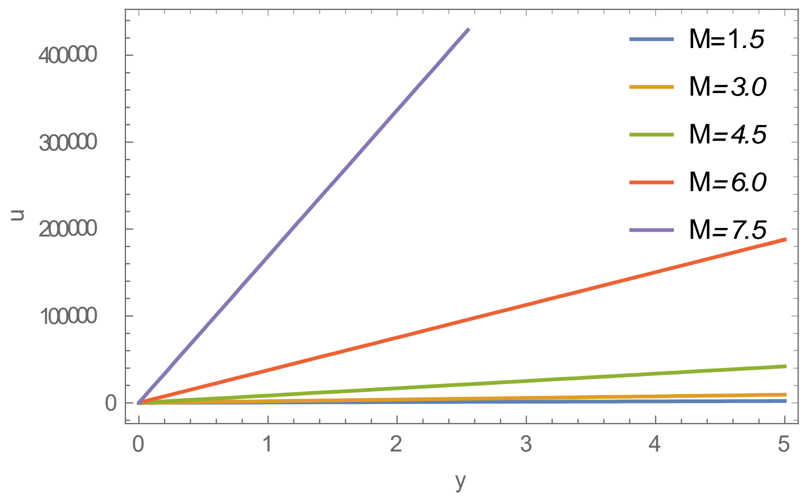

ISSN No. 2454-6194 | DOI: 10.51584/IJRIAS |Volume XI Issue VI June 2026

Figure 4: Velocity profile u against boundary layer y of electronic thermal system varying Hartmann number (M) when erfc = 0.1, Da = 1.8, Re = 2.

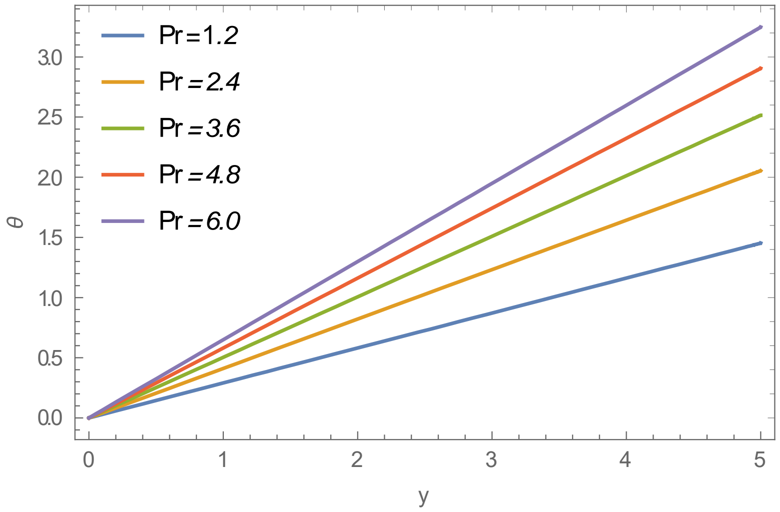

Figure 5: Temperature profile θ against boundary layer y of electronic thermal system varying Prandtl number when Rd = 1.8, Re = 2, erfc = 0.1.

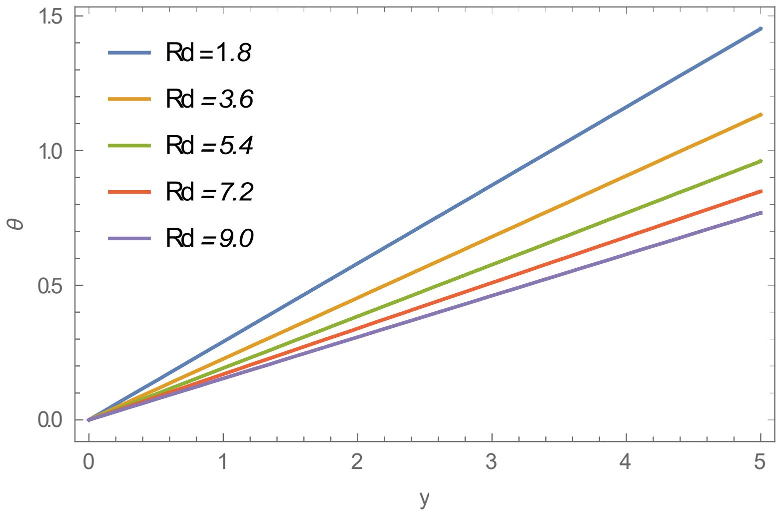

Figure 6: Temperature profile θ against boundary layer y of electronic thermal system varying Radiation parameter (Rd) when Pr = 1.2, erfc = 0.1.

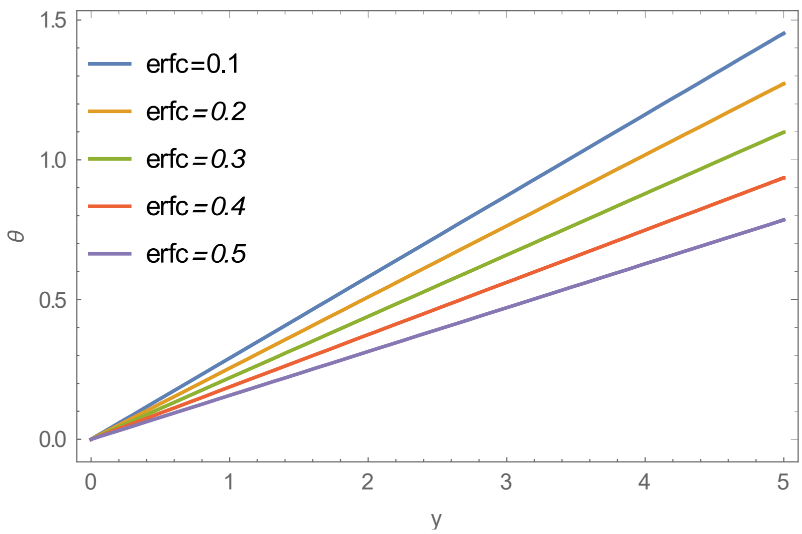

ISSN No. 2454-6194 | DOI: 10.51584/IJRIAS |Volume XI Issue VI June 2026

Figure 7: Temperature profile θ against boundary layer y of electronic thermal system varying complementary error function (erfc) when Pr = 1.2, erfc = 0.1.

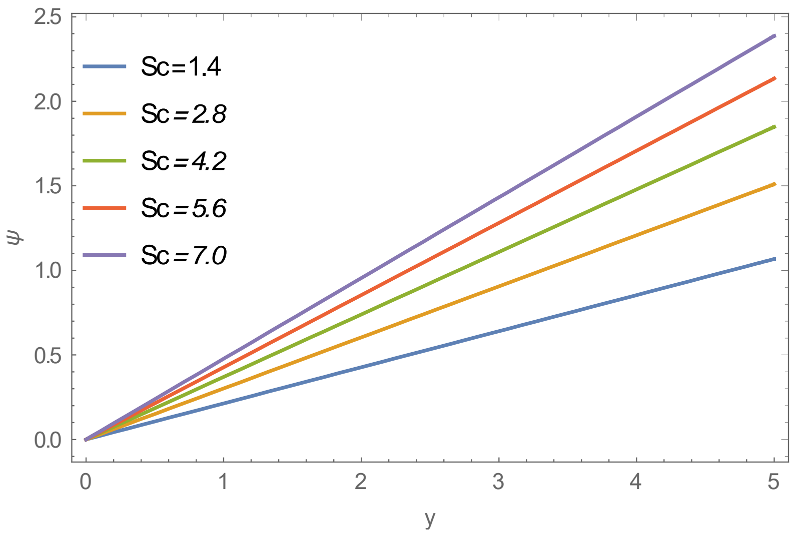

Figure 8: Concentration profile ψ against boundary layer y of electronic thermal system varying Schmidt number (Sc) when $\gamma = 0.9$, erfc = 0.1.

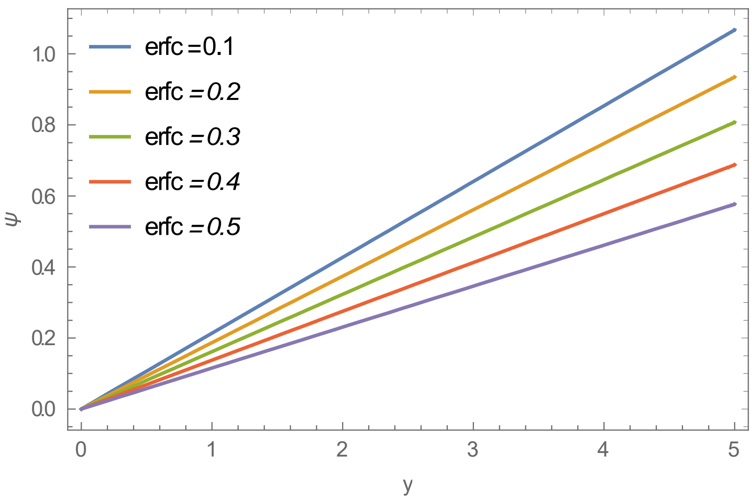

Figure 9: Concentration profile ψ against boundary layer y of electronic thermal system varying complementary error function (erfc) when $\gamma = 0.9$, Sc = 1.4.

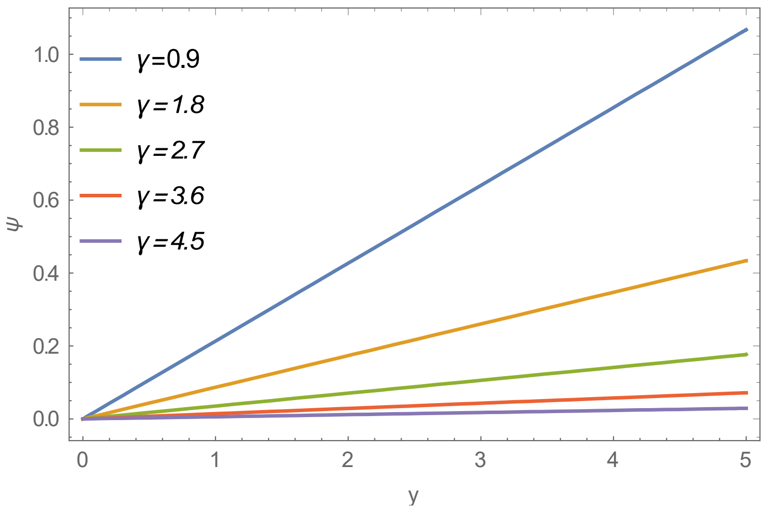

INTERNATIONAL JOURNAL OF RESEARCH AND INNOVATION IN APPLIED SCIENCE (IJRIAS)
ISSN No. 2454-6194 | DOI: 10.51584/IJRIAS |Volume XI Issue VI June 2026

Figure 10: Concentration profile ψ against boundary layer y of electronic thermal system varying Chemical reaction parameter (γ) when erfc = 0.1 0.9, Sc = 1.4.

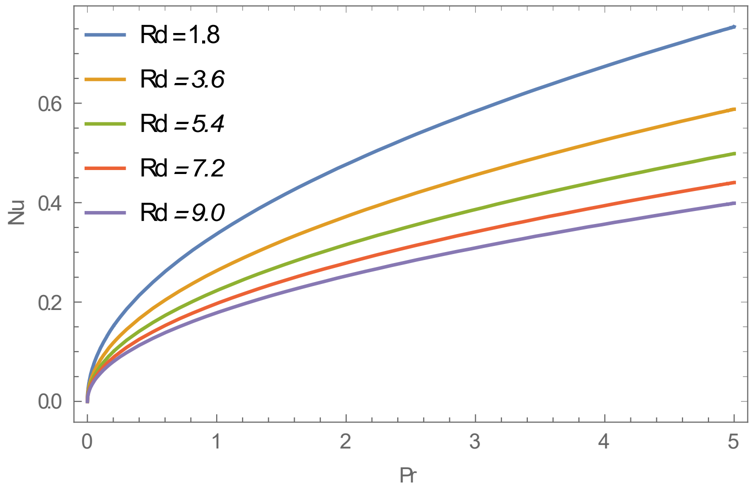

Figure 11: Nusselt number (Nu) against boundary layer of Prandtl number (Pr) with Radiation parameter term (Rd) varying.

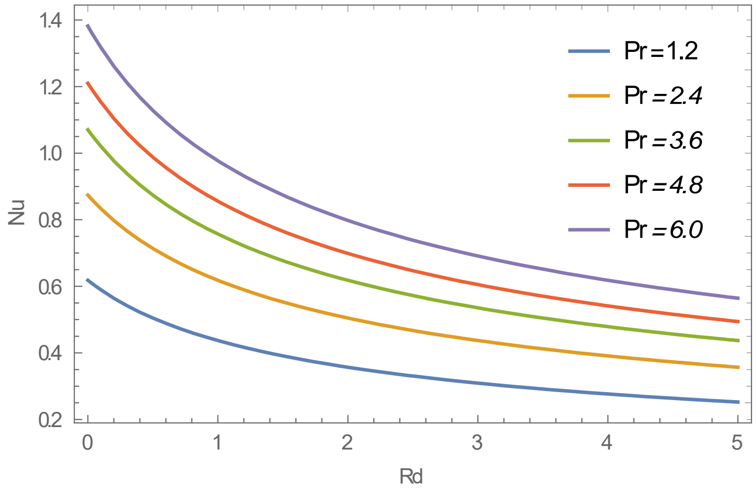

Figure 12: Nusselt number (Nu) against boundary layer of Radiation parameter term with Prandtl number (Pr) varying

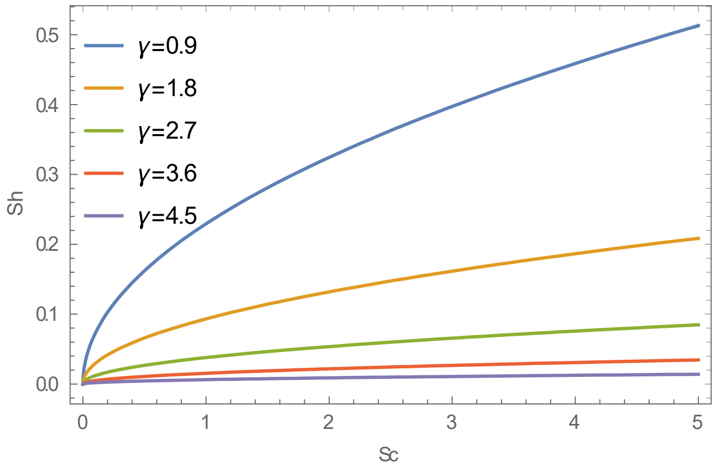

Figure 13: Sherwood number (Sh) against boundary layer of Schmidt number (Sc) with Chemical reaction (K_0) term varying.

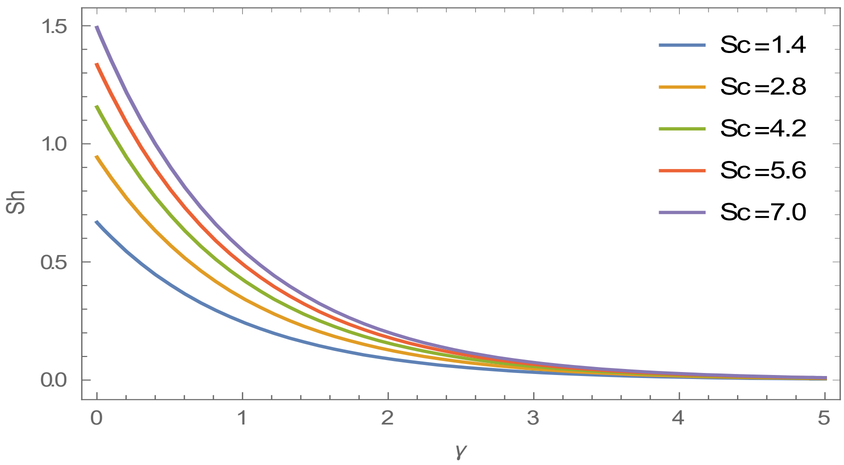

Figure 14: Sherwood number (Sh) against boundary layer of Chemical reaction (Rd) with Schmidt number (Sc) term varying.

Figure 1 illustrates the effect of Reynolds number (Re) on the velocity distribution of the magnetically controlled Fe_3O_4–water ferrofluid within the electronic thermal system. It is observed that increasing the Reynolds number significantly enhances the ferrofluid velocity throughout the cooling channel. Physically, higher Reynolds number corresponds to stronger inertial forces relative to viscous forces, thereby accelerating the fluid motion and reducing momentum diffusion within the boundary layer. Consequently, the velocity boundary layer thickness increases as (Re) rises. This behaviour is important in high-performance electronic cooling systems where rapid coolant circulation is required for efficient heat extraction from heat-generating electronic components such as microprocessors, integrated circuits, and power electronic modules.

Figure 2 presents the variation of velocity profile with increasing complementary error function (\operatorname{erfc}). The results indicate that larger values of (\operatorname{erfc}) enhance the transient velocity distribution within the ferrofluid flow region. This enhancement occurs because the complementary error function governs the diffusion characteristics associated with the analytical solution of the transport equations. The observed behaviour demonstrates improved transient momentum propagation within the cooling channel, which is beneficial in transient thermal management systems where rapid thermal response is essential for maintaining operational stability of electronic devices.

Figure 3 depicts the influence of Darcy number (Da) on the velocity distribution of the ferrofluid. It is evident that increasing Darcy number significantly increases the ferrofluid velocity. Physically, larger Darcy number corresponds to higher permeability of the porous medium, which reduces resistance to fluid motion and permits easier ferrofluid transport through the cooling substrate. The reduction in porous drag force enhances coolant penetration and circulation within the electronic thermal channel. This behaviour is particularly relevant in porous heat sinks, compact cooling chambers, and microchannel thermal systems where improved permeability contributes to efficient thermal regulation.

Figure 4 shows the effect of Hartmann number (M) on the ferrofluid velocity profile. The results reveal that increasing magnetic parameter suppresses the velocity distribution within the flow domain. This behaviour occurs due to the Lorentz force generated by the applied magnetic field, which opposes fluid motion and introduces electromagnetic damping within the conducting ferrofluid. As a result, momentum transport is reduced and the velocity boundary layer becomes thinner. This magnetic flow control mechanism is highly important in advanced electronic cooling systems, magnetic microfluidic devices, and electromagnetic thermal regulators where controlled coolant motion is required for precise thermal management.

Figure 5 illustrates the variation of temperature profile with increasing Prandtl number (Pr). It is observed that higher Prandtl number reduces the temperature distribution within the ferrofluid boundary layer. Physically, increasing (Pr) decreases thermal diffusivity relative to momentum diffusivity, thereby weakening heat propagation through the ferrofluid medium. Consequently, the thermal boundary layer thickness decreases significantly. This behaviour is relevant in electronic cooling applications involving highly viscous coolants

ISSN No. 2454-6194 | DOI: 10.51584/IJRIAS |Volume XI Issue VI June 2026

where thermal diffusion becomes limited and localized heating effects may occur within electronic components.

Figure 6 presents the influence of radiation parameter (Rd) on the temperature distribution of the ferrofluid. The results show that increasing thermal radiation parameter enhances the temperature profile throughout the cooling region. This occurs because thermal radiation contributes additional thermal energy to the ferrofluid system, thereby strengthening thermal diffusion and increasing thermal boundary layer thickness. The enhanced heat transport capability associated with larger radiation parameter improves thermal dissipation in high-temperature electronic systems such as semiconductor devices, power converters, and thermal energy storage modules.

Figure 7 demonstrates the effect of the complementary error function (\operatorname{erfc}) on the temperature distribution within the ferrofluid channel. It is observed that increasing (\operatorname{erfc}) enhances the transient thermal diffusion process and consequently increases the temperature distribution. The result confirms that the complementary error function plays a significant role in controlling transient heat transfer characteristics within the analytical model. This behaviour is important in transient electronic cooling operations where rapid thermal adjustment and efficient temperature regulation are required for maintaining system reliability.

Figure 8 illustrates the effect of Schmidt number (Sc) on the concentration profile of the ferrofluid system. It is observed that increasing Schmidt number reduces nanoparticle concentration distribution within the boundary layer. Physically, higher Schmidt number corresponds to lower mass diffusivity, which suppresses species diffusion within the ferrofluid channel. As a result, the concentration boundary layer thickness decreases significantly. This behaviour is important in nanoparticle transport regulation, reactive cooling systems, and ferrofluid concentration control applications used in electronic thermal devices.

Figure 9 presents the variation of concentration profile with increasing complementary error function (\operatorname{erfc}). The results indicate that increasing (\operatorname{erfc}) enhances the transient concentration diffusion process within the ferrofluid medium. This enhancement improves nanoparticle transport and species propagation throughout the cooling channel. The observed behaviour is useful in nanoparticle-assisted cooling technologies where controlled dispersion of magnetic nanoparticles contributes to enhanced thermal conductivity and improved electronic cooling efficiency.

Figure 10 shows the influence of chemical reaction parameter (\gamma) on the concentration distribution within the ferrofluid channel. It is observed that increasing chemical reaction parameter significantly reduces concentration profiles. Physically, stronger chemical reaction intensifies species consumption within the porous medium, thereby suppressing nanoparticle diffusion and reducing concentration boundary layer thickness. This behaviour is relevant in chemically reactive cooling systems and reactive ferrofluid applications where species depletion influences thermal transport efficiency and flow stability.

Figure 11 illustrates the variation of Nusselt number (Nu) with radiation parameter (Rd). The results reveal that increasing radiation parameter enhances the Nusselt number, indicating improved convective heat transfer at the channel surface. The increase in thermal radiation strengthens thermal energy transport within the ferrofluid system and consequently improves heat removal from the electronic surface. This behaviour demonstrates the importance of radiation-assisted ferrofluid cooling in advanced thermal management systems and high-power electronic devices.

Figure 12 depicts the effect of Prandtl number (Pr) on the Nusselt number. It is observed that increasing (Pr) increases the surface heat transfer rate despite reducing thermal boundary layer thickness. The enhancement in Nusselt number indicates stronger thermal gradients near the wall surface, thereby improving convective heat transfer efficiency. This behaviour is particularly significant in compact electronic cooling systems where efficient wall heat extraction is required for thermal protection of sensitive components.

Figure 13 presents the variation of Sherwood number (Sh) with chemical reaction parameter (\gamma). The results show that increasing chemical reaction parameter enhances the Sherwood number due to stronger concentration gradients near the wall surface. Physically, intensified chemical reaction accelerates species depletion within the ferrofluid medium and consequently increases mass transfer rates at the boundary surface. This behaviour is important in reactive nanoparticle transport systems and chemically controlled ferrofluid cooling technologies**.**

Figure 14 illustrates the influence of Schmidt number (Sc) on the Sherwood number. It is observed that increasing Schmidt number significantly enhances the Sherwood number within the ferrofluid system. Higher Schmidt number reduces species diffusivity and increases concentration gradients at the wall, thereby strengthening mass transfer rates. This behaviour is important in nanoparticle transport regulation, concentration stabilization, and controlled species diffusion processes within advanced electronic thermal management systems.

CONCLUSION

The present study successfully investigated the transport behaviour of magnetically controlled Fe_3O_4–water ferrofluid in an electronic thermal system under the combined influences of thermal radiation, porous medium resistance, and chemical reaction effects. The governing momentum, energy, and concentration equations were formulated using appropriate thermo-physical relations and solved analytically using the Laplace transform technique. The obtained results demonstrated the capability of the ferrofluid model in enhancing thermal regulation and controlling fluid transport within advanced electronic cooling systems.

- Increasing Reynolds number and Darcy number enhanced ferrofluid velocity due to reduction in viscous and porous resistance effects.
- Increasing Hartmann number suppressed the velocity distribution as a result of the Lorentz force generated by the applied magnetic field.
- Higher radiation parameter enhanced the temperature profile and improved thermal energy transport within the electronic cooling channel.
- Increasing Prandtl number reduced thermal boundary layer thickness due to lower thermal diffusivity of the ferrofluid.
- Larger Schmidt number and chemical reaction parameter reduced concentration distribution within the porous thermal system.
- The Nusselt number increased with thermal radiation and Prandtl number, indicating enhancement in convective heat transfer performance.
- The Sherwood number increased with Schmidt number and chemical reaction parameter due to stronger concentration gradients near the wall surface.
- The analytical results confirmed that Fe_3O_4–water ferrofluid possesses significant potential for application in electronic cooling devices, porous heat exchangers, microelectronic thermal systems, and electromagnetic thermal management technologies.

REFERENCES

1. Abareshi, M., Sajjadi, S. H., Zebarjad, S. M., & Goharshadi, E. K. (2011). Fabrication, characterization, and measurement of viscosity of α-Fe_2O_3–glycerol nanofluids. Journal of Molecular Liquids, 163(1), 27–32. https://doi.org/10.1016/j.molliq.2011.07.007
2. Choi, S. U. S., & Eastman, J. A. (1995). Enhancing thermal conductivity of fluids with nanoparticles. Proceedings of the ASME International Mechanical Engineering Congress and Exposition, 66, 99–105.

3. Cogley, A. C. L., Vincenti, W. G., & Gilles, S. E. (1968). Differential approximation for radiative transfer in a non-gray gas near equilibrium. AIAA Journal, 6(3), 551–553. https://doi.org/10.2514/3.4538
4. Eastman, J. A., Choi, S. U. S., Li, S., Yu, W., & Thompson, L. J. (2001). Anomalously increased effective thermal conductivities of ethylene glycol-based nanofluids containing copper nanoparticles. Applied Physics Letters, 78(6), 718–720. https://doi.org/10.1063/1.1341218
5. Farooq, U., Hassan, A., Fatima, N., Alghamdi, W., & Alshammari, F. (2023). A computational fluid dynamics analysis on Fe_3O_4–H_2O based nanofluid axisymmetric flow over a rotating disk with heat transfer enhancement. Scientific Reports, 13, 4679. https://doi.org/10.1038/s41598-023-31734-1
6. Ghadiri, M., Sardarabadi, M., Pasandideh-Fard, M., & Moghadam, A. J. (2015). Experimental investigation of hydrothermal characteristics of ferrofluids in a minichannel heat sink under magnetic field. Journal of Magnetism and Magnetic Materials, 381, 158–167. https://doi.org/10.1016/j.jmmm.2014.12.078
7. Guo, S. Z., Li, Y., Jiang, J. S., & Xie, H. Q. (2010). Nanofluids containing γ-Fe_2O_3 nanoparticles and their heat transfer enhancements. Nanoscale Research Letters, 5, 1222–1227. https://doi.org/10.1007/s11671-010-9630-1
8. Hassan, M. (2018). Impact of iron oxide particle concentration under oscillating magnetic field. The European Physical Journal Plus, 133, 230. https://doi.org/10.1140/epjp/i2018-12043-8
9. Karthikeyan, N. R., Philip, J., & Raj, B. (2008). Effect of clustering on the thermal conductivity of nanofluids. Materials Chemistry and Physics, 109(1), 50–55. https://doi.org/10.1016/j.matchemphys.2007.10.029
10. Sheikholeslami, M. (2019). Numerical investigation for second law analysis of ferrofluid inside a porous cavity with magnetohydrodynamic effect. Journal of Molecular Liquids, 295, 111534. https://doi.org/10.1016/j.molliq.2019.111534
11. Shima, P. D., Philip, J., & Raj, B. (2010). Synthesis of aqueous and nonaqueous iron oxide nanofluids and study of temperature dependence on thermal conductivity and viscosity. The Journal of Physical Chemistry C, 114(44), 18825–18833. https://doi.org/10.1021/jp107447q